Mitotic nuclear envelope breakdown and spindle nucleation are controlled by interphase contacts between centromeres and the nuclear envelope

Alfonso Fernández-Álvarez[1,2,*], **Cécile Bez**[2,3], **Eileen T. O'Toole**[4], **Mary Morphew**[4], and **Julia Promisel Cooper**[1,2,5,*]

[1]Telomere Biology Section, LBMB, National Cancer Institute, NIH, 9000 Rockville Pike, Bethesda, MD 20892, Phone 301-402-1530, FAX 301-402-3095

[2]Telomere Biology Laboratory, Cancer Research UK, London Research Institute, 44 Lincoln's Inn Fields, London, WC2A 3LY, UK

[4]Department of Molecular, Cellular, and Developmental Biology, University of Colorado, Boulder, CO 80309, USA

Summary

Faithful genome propagation requires coordination between nuclear envelope (NE) breakdown, spindle formation and chromosomal events. The conserved 'linker of nucleoskeleton and cytoskeleton' (LINC) complex connects fission yeast centromeres and the centrosome, across the NE, during interphase. During meiosis, LINC connects the centrosome with telomeres rather than centromeres. We previously showed that loss of telomere-LINC contacts compromises meiotic spindle formation. Here, we define the precise events regulated by telomere-LINC contacts and address the analogous possibility, that centromeres regulate mitotic spindle formation. We develop conditionally inactivated LINC complexes in which the conserved SUN-domain protein Sad1 remains stable but severs interphase centromere-LINC contacts. Strikingly, the loss of such contacts abolishes spindle formation. We pinpoint the defect to a failure in the partial NE breakdown required for centrosome insertion into the NE, a step analogous to mammalian NE breakdown. Thus, interphase chromosome-LINC contacts constitute a cell cycle control device linking nucleoplasmic and cytoplasmic events.

eTOC blurb

*Correspondence: alfonso.fernandezalvarez@nih.gov (A.F-A.) julie.cooper@nih.gov (J.P.C.).
[3]Current address: PRA Health Sciences-Paris, 92300 Levallois-Perret, France.
[5]Lead Contact: Julia Promisel Cooper

The role of interphase centromere-LINC contacts has been a longstanding intractable mystery. Fernández-Álvarez et al. generate a mutation that severs these centromere-LINC contacts, leading to failed nuclear envelope breakdown, and in turn, failed spindle assembly. Thus, centromere-LINC contacts couple chromosomal events with cytoplasmic events that propel the cell cycle.
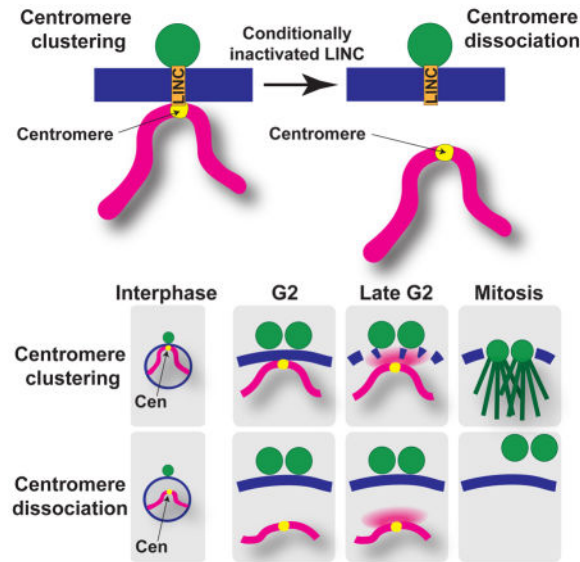
INTRODUCTION

Centrosomes are the major microtubule-organizing center in the cell, participating in a number of critical processes such as bipolar spindle formation, morphogenesis and cell motility (Bettencourt-Dias and Glover, 2007; Gould and Borisy, 1977; Mardin and Schiebel, 2012). During cell proliferation, a precise succession of events affords centrosome duplication and separation, once per cell cycle, to ensure equal chromosome segregation; problems in this succession result in genetic instability and tumorigenesis (Basto et al., 2008; Ganem et al., 2009; Gonczy, 2015). Crucially, the metazoan centrosome cycle is coordinated with nuclear envelope breakdown (NEBD), in which the entire NE is dissolved to allow chromosomes to access their segregation vehicle, the spindle (Guttinger et al., 2009). In fission yeast, complete NEBD is replaced by a localized disassembly (fenestration) of the nuclear envelope (NE) beneath the centrosome (called the spindle pole body or SPB). This partial NEBD creates an interruption in the NE into which duplicated SPBs descend at the onset of mitosis; SPB insertion is followed by intranuclear spindle formation (Ding et al., 1997).

NEBD is also essential for faithful chromosome segregation in meiosis (Pfender et al., 2015), the specialized cell cycle in which two rounds of nuclear division follow a single round of DNA replication, giving rise to haploid gametes and driving sexual reproduction (Petronczki et al., 2003; Yanowitz, 2010). We previously demonstrated that trans-NE contacts between chromosomes and the centrosome control meiotic spindle formation in fission yeast (Tomita and Cooper, 2007). This observation stemmed from studying the function of the telomere bouquet, a widely conserved meiotic prophase-specific

chromosomal arrangement in which telomeres cluster together at the NE beneath the SPB (Klutstein and Cooper, 2014; Scherthan, 2001). The linkage between the telomere bouquet and the SPB (on the outer surface of the NE during meiotic prophase) occurs *via* the LINC complex, which comprises the KASH-domain outer NE protein Kms1 and the SUN-domain inner NE protein Sad1. The meiotic prophase-specific Bqt1/2 complex, which binds both Sad1 and the constitutively telomere-bound Taz1/Rap1 complex (Chikashige et al., 2006), completes the telomere-LINC connection. The bouquet persists throughout meiotic prophase, a period during which the SPB is pulled back and forth along cytoplasmic microtubules; this oscillatory movement, along with the LINC-mediated association between telomeres and the SPB, gives rise to the elongated 'horsetail' nuclear shape (Figure 1A) (Ding et al., 1998). The cessation of horsetail movements is followed by SPB duplication and insertion of mother and daughter SPBs into the NE. This insertion sets the stage for recruitment of the nuclear γ-tubulin complex (γ-TuC), which nucleates spindle formation (Funaya et al., 2012).

In our studies of telomeric control of meiotic spindle formation, we found that cells lacking telomere-SPB linkages can successfully form spindles if centromere-SPB contacts occur in their stead (Fennell et al., 2015). Indeed, association of only a single telomere (Tomita et al., 2013) or centromere (Fennell et al., 2015) with LINC is sufficient to ensure spindle assembly. This shared meiotic spindle-promoting ability of telomeres and centromeres, along with the presence of centromere-LINC contacts beneath the SPB during mitotic interphase (Funabiki et al., 1993), raised the possibility that centromeres regulate mitotic spindle formation in a manner analogous to the role of telomeres in meiosis. However, this possibility has heretofore been difficult to address, as complete disruption of interphase centromere-LINC associations could not be achieved without compromising several variables. For instance, mutations in kinetochore factors like Nuf2 or Cnp1 compromise centromere-LINC association in interphase, but also compromise additional aspects of kinetochore function, making it impossible to attribute the effects of *nuf2* or *cnp1* mutations to loss of interphase centromere-LINC connections (Asakawa et al., 2005; Takahashi et al., 2000). Other mutations, like that of the LINC-interacting factor Csi1, only partially disrupt centromere clustering beneath the SPB (Hou et al., 2012). Given the aforementioned observation that contact between a single centromere or telomere and the LINC complex is sufficient to confer proper meiotic spindle formation, disruption of chromatin-LINC associations likely need to be complete in order to reveal any role of such association in mitotic spindle formation.

Here, we define which events in the pathway to spindle assembly are compromised in cells lacking meiotic telomere-LINC contacts, and definitively show that analogous processes connect chromosome contacts with mitotic spindle formation as well. To investigate mitosis, we developed a mutation conferring release of all centromeres from their normal LINC association during interphase. In this scenario, SPB and spindle defects mimicking those seen in bouquet-defective meiosis are seen at mitosis. While SPB duplication proceeds unhampered in the absence of telomere- or centromere-LINC contacts, insertion of the SPB into the NE requires these contacts. Our observations reveal an active role of chromosomes in mediating NE disassembly at the onset of mitosis and thereby coupling the spatial

chromosome configuration inside the nucleus with the cytoplasmic events required for spindle nucleation.

RESULTS

Telomere-LINC contacts are required for SPB separation during meiosis

To pinpoint which steps in the meiotic centrosome cycle require chromatin-LINC association, we analyzed the dynamics of several SPB components in live *wt* and bouquet defective (*bqt1*) cells, starting with the pericentrin ortholog Pcp1, the core SPB component that recruits the γ-TuC to nucleate spindle formation (Fong et al., 2010). Pcp1 first appears in a conspicuous focus in late prophase (~20 minutes before meiosis I (MI)), when it separates along with the SPB into two clear foci; the cycle is repeated at meiosis II (MII), leading to four Pcp1 foci (Figure 1B). In contrast, in the absence of the bouquet, the duplicated SPBs often fail to separate (Figure 1C). Indeed, 75.5% of *bqt1* cells with defective meiosis show problems in SPB separation at MI; the remaining 24.5% display normal SPB separation at MI but defective separation at MII (n=57).

SPB separation requires spindle elongation, which pushes the duplicated SPBs apart (Lim et al., 2009). As the γ-TuC is a key player in nucleating both cytoplasmic microtubules and spindles (Job et al., 2003), we probed whether the γ-TuC is recruited to the SPBs in bouquet-deficient settings by monitoring Alp4, an essential component of the γ-TuC (Vardy and Toda, 2000). Alp4 localizes to the SPB throughout *wt* meiosis ((Tanaka et al., 2005); Figure 1D). In contrast, Alp4 localization is defective (ie one or both SPB signals lack any detectable Alp4 colocalization at MI onset) in 59% of *bqt1* meiocytes (n= 100, p<0.01) from the onset of MI onwards, and all (n=50, p<0.01) those SPBs failing to recruit Alp4 show SPB separation problems and failed spindle nucleation (Figure 1E). Hence, the bouquet is required for γ-TuC recruitment as well as spindle nucleation and SPB separation.

SPB duplication occurs independently of telomere-LINC contacts

What molecular alterations might underlie the SPB separation and γ-TuC recruitment defects triggered by bouquet disruption? Pcp1 overexpression causes SPB and spindle defects (Fong et al., 2010; Jin et al., 2005), raising the possibility that lack of contact with the bouquet confers an over-accumulation of SPB components. To address this possibility, we quantified the focal intensity of Pcp1-GFP through meiosis. In *wt* meiocytes, Pcp1 intensity follows a dynamic curve that can be subdivided into three phases (Figure S1A). First, Pcp1 accumulates during late prophase when the bouquet is present (Ohta et al., 2012). The second phase begins with a shoulder starting at MI onset when the bouquet has dissolved, SPB duplication has finished, and the MI spindle forms and segregates homologs. The shoulder stage is followed by a steep climb in intensity corresponding to the second meiotic SPB duplication. The peak of the curve corresponds to MII spindle formation and sister chromatid segregation, and is followed by the diminution of Pcp1 signal as meiosis concludes (Figure S1A). Perhaps surprisingly, Pcp1 dynamics are similar through *wt* and *bqt1* meiosis (Figure S1A). Although very modest increases in Pcp1 level at the shoulder and peak of the curve are seen in the absence of the bouquet, we found that subtle over-

expression of Pcp1 (i.e. to a magnitude similar to that in the *bqt1* setting) fails to confer SPB or spindle defects (Figure S1B).

To determine whether Pcp1 accumulation reflects the SPB as a whole, we quantified the levels of the additional integral components Sid4, Cut11 and Cut12 (Bridge et al., 1998; Chang and Gould, 2000; West et al., 1998). As for Pcp1, the timing and extent of accumulation of all three are similar in *wt* and spindle-deficient *bqt1* meiosis (Figure S1C–E). Furthermore, despite differences in their meiotic dynamics, Pcp1 (which accumulates dramatically at MI onset) and Sid4 (which accumulates gradually prior to MI onset (Ohta et al., 2012)) always colocalize in both *wt* and *bqt1* meiocytes (Figure S1F and S1G). Hence, failed γ-Tuc recruitment and spindle nucleation in the *bqt1* setting is not due to failed SPB duplication.

Mitotic SPB duplication is a conservative process that results in distinguishable old and new SPBs (Flory et al., 2002; Grallert et al., 2004; Pereira et al., 2001; Tallada et al., 2009). To determine whether old and new SPBs can be distinguished during meiosis, and if so, whether the old or new SPB is more prone to fail in the absence of the bouquet, we monitored the fluorescence of a fusion between a slow-folding DsRed variant (sfRFP, which takes ~11 hours to fold into active form) and Pcp1. In cells arrested in G1 (ie, with unduplicated SPBs) for 12 hours by nitrogen starvation, the majority of Pcp1-sfRFP molecules have folded properly and the SPB fluoresces (−60′ and −70′ in Figure S1H and S1I, respectively). Upon subsequent induction of meiosis, the SPB duplicates, but only one of the two SPBs is visible *via* the sfRFP tag, indicating that as in mitosis, meiotic SPB duplication yields distinguishable old (containing pre-folded Pcp1-sfRFP) and new (containing a not-yet-folded sfRFP moiety fused with Pcp1) SPBs. In 100% of the *bqt1* cells that show monopolar spindles (n=11), those spindles are nucleated specifically from the old SPB (Figure S1I). Hence, failed spindle nucleation in the absence of the bouquet is specific to the new SPB.

Telomere-LINC contact is required for SPB insertion into the NE

We previously observed a tendency for the SPB to dissociate from the NE just prior to meiotic spindle formation in the *bqt1* setting (Fennell et al., 2015; Tomita and Cooper, 2007); indeed, SPBs showing problems in separation typically appear to dislodge into the cytoplasm (Figure 1C, yellow arrowheads). This separation of the SPB from the NE can be seen clearly using the tagged transmembrane protein Ish1, which localizes throughout the NE (Figure 1F and 1G). As shown previously, the SPB remains associated with the NE throughout prophase in both *wt* and *bqt1* meiocytes. Indeed, regardless of bouquet formation or failure, the SPB remains associated with the NE throughout the horsetail movement stage and for ~40 minutes after movements have ceased (Figure 1F and 1G); only after the ensuing SPB duplication do the SPBs dislodge from the NE (Figure 1G).

To clarify this phenotype in greater detail, we subjected *wt* and *bqt1* cells to high-pressure freezing and freeze substitution followed by serial sectioning and electron microscopy (EM). A representative image of a *wt* MII cell reveals two electron-dense SPBs at opposite ends of a nucleus (Figure 1H); at this stage, each SPB has nucleated a clearly visible pro-spore membrane (PSM, Figure 1H). An example of a MII *bqt1* cell reveals that two SPBs, the

NE and two PSMs are easily recognized, reaffirming that SPB duplication occurs in the absence of the bouquet; moreover, both SPBs remain sufficiently functional to nucleate PSMs. However, one of the two SPBs has clearly dislodged from the NE (upper left SPB in Figure 1I). By capturing images at varying tilt angles and performing tomographic reconstruction, we confirmed that the inserted SPB nucleates a classic monopolar spindle whose morphology contrasts with that of a bipolar spindle; while the latter comprises aligned overlapping microtubules, monopolar spindles comprise an excessive number of microtubules splayed at varying angles (Figure S2; Movies S1–2). In contrast, the SPB that fails to insert also fails to nucleate spindle microtubules (Figure S2; Movies S1–2).

A Sad1 mutant protein that confers SPB-centromere dissociation during mitotic interphase

The myriad analogies between mitotic and meiotic progression, from the shared need for NE fenestration and SPB insertion to the shared presence of LINC-chromatin contacts (*via* telomeres in meiotic prophase or centromeres in mitotic interphase), prompt the question of whether chromosomal control of spindle formation applies not only to meiosis, but also to proliferative cell cycles. To develop a system that affords complete dissociation of interphase centromeres from the LINC complex, we generated a conditional Sad1 mutant. We first generated a series of nested deletions (Figure 2A) in the nucleoplasmic domain of Sad1 and used this series to identify the region, amino acids 2–60, that confers centromere-LINC associations (Figures 2B and S3A–E). Based on this information, we constructed a library of Sad1 alleles in which the first 60 amino acids were randomly mutated and the C-terminus was GFP-tagged, replaced *sad1+* with these alleles in an otherwise *wt* background, and screened for temperature sensitive growth (Figure 2B). As we sought mutations affecting the interphase association of centromeres with Sad1 without compromising its stability or localization, mutations affecting Sad1 intensity at the SPB at 25°C or 36°C were discarded. This approach identified a Sad1 *ts* allele dubbed *sad1.2*, which harbors two substitutions: threonine to serine at position 3, and serine to proline at position 52. Sad1.2 confers growth comparable to *wt* at the permissive temperature of 25°C; however, growth is abolished at 36°C (Figure 2C). This phenotype contrasts with the previously identified *ts* allele *sad1.1,* which encodes an alanine to valine substitution at position 323 in the SUN-domain and compromises growth at all temperatures (Fennell et al., 2015; Hagan and Yanagida, 1995).

Single Thr-3-Ser or Ser-52-Pro substitutions fail to phenocopy *sad1.2* (Figure 2D). Ser52 is phosphorylated in a cell cycle dependent manner (Carpy et al., 2014), raising the possibility that this modification plays a role in cell cycle progression. However, as Ser-52-Ala fails to reproduce the effect of Ser-52-Pro in combination with Thr-3-Ser, phosphorylation alone is unlikely to explain the effects of Ser52 mutation in the context of *sad1.2*. Similarly, T3A in combination with S52P fails to recreate the *sad1.2* phenotype, and various combinations of substitutions to alanine or glutamic acid at either position yield only partial growth defects, with the exception of simultaneous Thr-3-Glu and Ser-52-Ala substitution (Figure 2D). Hence, while compromised Sad1 phosphorylation may contribute to the *sad1.2* phenotype, constitutive conformational alterations are likely to play a prominent role.

In accord with our screening criteria, Sad1.2-GFP remains stably associated with the SPB throughout interphase, in contrast to Sad1.1-GFP, which is destabilized at 36°C (Figure 3A).

Moreover, Sid4 and Pcp1 show comparable intensities in *sad1.2 versus wt* settings, at both 25°C and 36°C (Figures 3B–C, S4A); hence, neither LINC nor SPB stability are perturbed in *sad1.2* cells. Moreover, the inner NE proteins Lem2 and Man1 show no conspicuous differences in localization in *wt versus sad1.2* cells at 36°C, suggesting that the NE remains largely unperturbed (Figure S4B).

The LINC and SPB stability of *sad1.2* cells allowed us to address the possibility that defects in centromere-LINC clustering underlie the reduced viability of these cells. Hence, we evaluated centromere localization in proliferating cells. While all kinetochore (Mis6) signals localize to a single bright focus beneath the SPB during *wt* interphase, *sad1.2* cells often show extra Mis6-GFP foci unassociated with the SPB, even at permissive temperature. At restrictive temperature, a population of *sad1.2* cells emerges in which all three centromeres are clearly dissociated from the SPB (Figure 3D). To further define these phenotypes, we categorized cells according to the position of centromeres with respect to the interphase SPB, scored during the 40 min prior to SPB duplication: 1) *wt-like*, in which all centromeres cluster at the SPB; 2) *partial dissociation*, in which at least one centromere localizes to the SPB but additional centromere foci localize elsewhere; and 3) *total dissociation*, in which all centromere foci are separated from the SPB (Figure 3D). At permissive temperatures (25°C or 32°C), ~80% of *sad1.2* cells show *partial dissociation* and none show *total dissociation*. In contrast, after 4 h at 36 °C, ~20% of *sad1.2* cells show *total dissociation*. Longer incubation times at 36 °C increase the proportion of cells showing *total dissociation* (Figure 3E).

Centromere-LINC association during mitotic interphase is required for spindle formation

If interphase centromere-LINC associations play a mitotic role analogous to that of telomere-LINC associations in meiotic spindle formation, *total centromere dissociation* should be analogous to complete bouquet disruption, which confers defective meiotic spindle formation; in contrast, association of even a single centromere with the SPB would suffice in promoting spindle formation (Fennell et al., 2015). Analysis of the spindle behavior associated with each *sad1.2* category reveals that all cells displaying at least one interphase centromere-LINC contact (*wt-like* and *partial dissociation* categories) form proper spindles (Figure 3F; Figure S4D and S4E), in accord with our observations that a single telomere- or centromere-SPB interaction bestows meiotic spindle formation. In striking contrast, 100% of the *sad1.2* cells with *total centromere dissociation* in interphase fail in spindle formation (Figure 3F and Figure S4F).

The details of failed mitotic spindle formation following interphase in the absence of centromere-LINC interaction are nearly identical to those of failed meiotic spindle formation in the absence of telomere/centromere-LINC contacts in the preceding prophase. As in bouquet-defective meiotic cells, *sad1.2* cells experiencing *total centromere dissociation* are able to accomplish proper SPB duplication (Figure 4B). However, these cells fail at the NE insertion step. While in a *wt* setting, the duplicated SPBs insert into the NE just prior to the onset of spindle formation (Ding et al., 1997; Tallada et al., 2009; McCully and Robinow, 1971; Tanaka and Kanbe, 1986), the SPBs of *sad1.2* cells exhibiting *total centromere dissociation* not only fail to insert but also appear to separate from the NE, dislodging into the cytoplasm (Figures 4D–E, S5B, S5D); this behavior is identical to that observed in

meiotic cells lacking telomere- and centromere-LINC association (Figure 1G, I). Moreover, as was seen for bouquet-defective meiosis, the SPB remains associated with the outer NE throughout interphase in the *sad1.2* setting; only after SPB duplication, when the NE should form a fenestration allowing SPB insertion, does the SPB separate from the NE (Figure 4D; Figure S5B and S5D). These observations suggest NE remodeling, and/or modification of factors that signal the onset of SPB insertion, as the initial centromere-LINC contact-mediated parameter controlling spindle formation.

The consistency of our results using different tagged kinetochore proteins as centromeric markers (Figure S5F), together with the fact that *sad1.2* cell viability is preserved at 32 °C despite *partial centromere dissociation* in ~75% of cells, confirms that kinetochores remain intact despite their LINC delocalization in the *sad1.2* setting. Likewise, centromeric silencing remains intact in a setting of *partial centromere dissociation* from the SPB; note that silencing in the *total dissociation* scenario cannot be assessed as it leads to inviability. Hence, localization of centromeres to the SPB is dispensable for the maintenance of pericentric heterochromatin (Figure S5G). Conversely, histone H3-Lys9 (H3-K9) methylation, a hallmark of heterochromatin, is dispensable for the ability of centromeres to contact the LINC complex and confer proper spindle formation, as loss of the sole H3-K9 methyltransferase (Clr4) has no impact on either variable (Figure S5H, (Fennell et al., 2015)). This observation recalls previous work showing that while pericentric heterochromatin is required for *establishment* of centromeric CenpA and kinetochore function on naïve sequences, CenpA and kinetochores can be *maintained* indefinitely in the absence of pericentric heterochromatin (Folco et al., 2008); like centromere identity itself, the ability to confer proper SPB insertion and spindle formation is maintained independently of H3-K9 methylation.

Centromere-LINC interactions and spindle rescue in *bqt1*Δ meiosis are abolished in a *sad1.2* background

While centromeres remain associated with LINC throughout *wt* mitotic interphase, they dissociate once the bouquet forms and nuclear oscillations commence in meiotic prophase (Klutstein et al., 2015); centromeres are also released from LINC in bouquet-defective cells (Figure 5B; (Cooper et al., 1998; Tomita and Cooper, 2007)). The *sad1.2* mutation has no impact on bouquet formation (Figure 5C); hence, the indirect Bqt1/Bq2-mediated linkage between meiotic telomeres and Sad1 requires different Sad1 residues than those involved in mitotic centromere interactions. Accordingly, spindle formation occurs normally at both MI and MII in *sad1.2* meiosis (Figure 5C). As single centromeres often sporadically reassociate with the SPB in bouquet-deficient meiosis and in doing so, rescue spindle formation (Fennell et al., 2015), we investigated whether such centromere reassociation events are altered by the *sad1.2* mutation. Indeed, we failed to observe any centromere-SPB contacts during meiotic prophase in either *sad1.2* or *bqt1*Δ *sad1.2* settings (Figure 5C–5E). Accordingly, proper meiotic spindle formation is completely abolished in the *bqt1*Δ *sad1.2* double mutant (Figures 5D and 5F). Hence, not only are Sad1–T3 and –S52 essential for mitotic centromere clustering, but also these residues are responsible for sporadic meiotic prophase centromere-LINC interactions and the associated rescue of *bqt1*Δ spindle failure.

Forced centromere-Sad1.2 association fully rescues spindle formation

The perfect correlation between spindle failure and *total centromere dissociation* strongly suggests that abolition of centromere association is specifically responsible for *sad1.2*-induced spindle failure. To evaluate the possibility, albeit unlikely, that *sad1.2* spindle failure stems from alternative problems (eg defects in Sad1 that are independent of its association with centromeres), we queried whether *sad1.2* spindle failure could be ameliorated by re-localizing centromeres to the LINC complex in a *sad1.2* setting. Hence, we utilized the GFP binding protein, GBP, to recruit GFP-tagged proteins (Rothbauer et al., 2006) to Sad1.2 (Figure 6A). In meiotic cells lacking Bqt2, Bqt1 localizes exclusively to SPB-associated Sad1 foci (Chikashige et al., 2006). Therefore, expression of Bqt1 in mitotic cells, which lack Bqt2, should result in binding of Sad1 by Bqt1, making Bqt1-GBP an effective tool for GBP-GFP-mediated recruitment of centromeres to Sad1; this strategy seemed particularly feasible given that Sad1.2 retains the ability to bind Bqt1/2 and confer bouquet formation (Figure 5C). Indeed, mitotically expressed Bqt1-GBP co-localizes with Sad1 in interphase (Figure 6B).

In *sad1.2* cells harboring Mis6-GFP but lacking mitotic Bqt1-GBP, failed centromere-LINC association leads to failed mitotic spindle formation, as described above (Figure 6C). However, induced expression of Bqt1-GBP in these cells confers efficient recruitment of centromere-bound Mis6-GFP to the SPB; at least one centromere stably interacts with the interphase SPB despite transfer to non-permissive temperature (Figure 6D and 6H). Remarkably, this stable centromere association rescues proper bipolar spindle formation (Figure 6D and 6I) and viability (Figure 6J) in the *sad1.2* setting. Likewise, meiotic (ie, endogenously expressed) Bqt1-GBP confers Mis6-GFP mediated centromere recruitment in bouquet-deficient (*rap1*Δ) *sad1.2* meiocytes, conferring proper meiotic spindle formation (Figure 5E and 5G).

To further probe the observation that ectopic targeting of centromeres to Sad1.2 rescues its inability to promote spindle formation, the Sad1-interacting factor Csi1, whose association with Sad1 is unaltered by the *sad1.2* mutations (Figure 3A), was endogenously fused with GBP. As seen for Bqt1-GBP, Csi1-GBP promotes efficient recruitment of centromeres (*via* Mis6-GFP) to Sad1.2 and rescues both spindle formation and cell viability (Figure 6E and 6J). Moreover, utilization of a different centromeric tag, a GFP-Lac repressor-bound *lacO* array inserted adjacent to centromere I, also results in localization of *cenI* to Sad1.2-associated Bqt1-GBP (Figure 6G and 6H) and restores both spindle formation and cell viability (Figure 6G, 6I and 6J). Hence, the spindle failure and viability loss conferred by Sad1.2 can be directly attributed to loss of interphase centromere-LINC contacts.

Interphase centromere-LINC association drives NE disassembly at mitotic onset

As interphase centromere-LINC contacts are required for SPB insertion into the NE, these contacts may control one or both of two processes. First, they may control the NE remodeling process that comprises fenestration. Second, they may control SPB modifications required for insertion into NE fenestra. Hence, a key question is whether NE fenestration occurs in the absence of centromere-LINC contact. NE fenestration is difficult to capture by microscopy as it is exceedingly rapid and transient (Ding et al., 1997; Tallada

et al., 2009). To overcome this limitation, we used efflux of a nuclear GFP marker (NLS-GFP-β-Gal) as a proxy for NE fenestration. Such efflux is so transient that it cannot be seen in *wt* proliferating cells. However, *cut11.1*, which encodes a mutation in the fission yeast ortholog of metazoan Ndc1, confers failed SPB insertion and arrest at the fenestration stage at 36°C, prolonging the period in which NLS-GFP-β-Gal can be seen to disappear from the nucleoplasm and appear in the cytoplasm to ~25 minutes (Tallada et al., 2009; Yoshida and Sazer, 2004) (Figure 7B). Indeed, while NLS-GFP-β-Gal cannot be seen to leave the nucleus through the *wt* mitotic cycle, efflux is clearly seen just after the duplicated SPBs begin to separate in the *cut11.1* setting. In contrast, *sad1.2* cells grown at 36°C for 8 hours show no indication of NLS-GFP-β-Gal efflux, despite failure to insert the duplicated SPBs (Figure 7C). Remarkably, introduction of the *sad1.2* mutation strongly averts the nuclear efflux phenotype of *cut11.1* cells (Figure 7D and 7E). Moreover, the residual level of *cut11.1 sad1.2* cells showing nuclear efflux is consonant with the residual level of *sad1.2* cells showing partial centromere dissociation after 8 hours at 36°C. Remarkably, the forced centromere association afforded by the Csi1-GBP/Mis6-GFP tethering system restores nuclear efflux to *cut11.1 sad1.2* cells (Figure S6). Hence, interphase centromere-LINC contacts are crucial for driving the NE disassembly required for SPB insertion.

DISCUSSION

Chromosomal control of NEBD – a cell cycle regulatory module uncovered by a precision tool

Here we reveal a regulatory module in which interphase centromeres coordinate the ability of cytoplasmic centrosomes to access the nucleus and thereby control spindle formation and cell cycle progression. This chromosome-cytoplasm coordination module is conserved from meiosis to mitosis, with the key difference that meiotic cells choose telomeres as the chromosomal contact point while mitotic cells choose centromeres. Meiotic cells experiencing loss of prophase telomere-LINC contacts accomplish SPB duplication, but the duplicated SPBs neither insert into the nucleus nor recruit the γ-TUC to nucleate spindles. Likewise, mitotic cells lacking interphase centromere-LINC contacts undergo SPB duplication but suffer SPB dissociation from the NE at the very stage during which the SPB pair should insert. Our observation that *sad1.2* blocks the prolonged NE permeability conferred by *cut11.1* mutation implicates NE fenestration as the pivotal step requiring centromere-LINC contact. Indeed, our data raise the possibility that chromosome contacts trigger not only the partial NEBD represented by NE fenestration, but also the complete NEBD seen at each mammalian cell division.

Development of a precision tool for specifically disrupting centromere-LINC contacts, against the backdrop of an intact and properly localized LINC complex, was crucial for delineating the role of such contacts. The cause/effect relationship between *total centromere dissociation* and *sad1.2* lethality is demonstrated not only by the observation that *sad1.2* cells showing *partial centromere dissociation* show *wt* spindle formation and cell cycle progression, but also by the rescued spindle formation and viability conferred by artificially re-tethering centromeres to Sad1.2. Meiotic telomere bouquet formation is unaffected by *sad1.2*, underlining the specificity of this allele for disrupting centromere-LINC association.

Moreover, the abolition of centromere-LINC interactions by *sad1.2* leads to fully penetrant spindle defects in meiotic cells lacking the telomere bouquet. The completeness of the *sad1.2 bqt1* meiotic phenotype, as well as the mitotic *sad1.2* single mutant penetrance, open up new horizons for screens to fully delineate the mechanisms coupling centromeres and telomeres with NE fenestration and spindle assembly.

The continuum of NE disassembly through eukarya

Controlled NE disassembly at the onset of nuclear division is a conserved process whose extent varies along a continuum across eukaryotes (Guttinger et al., 2009; Smoyer and Jaspersen, 2014), with mitosis being classified as *open*, *semi-open* and *closed* (Makarova and Oliferenko, 2016; Sazer et al., 2014). In most metazoans including vertebrates, complete NEBD occurs at the prophase-prometaphase stage and involves the disassembly of nuclear pore complexes (NPCs), lamins, and outer and inner nuclear membranes, whose components are redistributed throughout the endoplasmic reticulum and cytoplasm. Many fungi, including *S. cerevisiae*, display a *closed* mitosis and resolve the problem of uniting chromosomes with spindles by embedding SPBs in the NE as they assemble; hence, budding yeast SPBs span the outer and inner nuclear membranes throughout the cell cycle (Jaspersen and Ghosh, 2012). Nevertheless, even in this extreme case, NE remodeling accompanies SPB insertion as reflected by the competition between SPBs and NPCs for NE remodeling factors, and the NPC reorganization required for SPB insertion (Friederichs et al., 2011; Witkin et al., 2010). Further along the continuum, NPCs of the filamentous fungus *Aspergillus nidulans* disassemble partially, with several nucleoporins dispersing from the NE to the cytoplasm at mitotic onset, even though the NE remains largely intact; this NPC disassembly is thought to promote access of tubulin and mitotic regulators to the nucleus (De Souza et al., 2004). The *S. pombe* NE is further yet along the continuum, showing local disassembly in a rapid process that creates a NE hole large enough to accommodate both SPB insertion and access of cytoplasmic tubulin to the nucleus (Ding et al., 1997; Tallada et al., 2009; Tamm et al., 2011). Such local NE disassembly is also seen in some metazoans; in *Drosophila melanogaster* embryos, the NE is disrupted only at the poles at the onset of nuclear division (Katsani et al., 2008; Kiseleva et al., 2001; Paddy et al., 1996; Stafstrom and Staehelin, 1984). We speculate that contacts between centromeres or telomeres and the NE are utilized to couple nuclear events to NEBD, whether partial or complete, in a wide variety of eukaryotes, as discussed below.

Control of the onset of NEBD and spindle activation

Although the pathways controlling NEBD onset are far from understood, it is known that kinases like the cyclin-dependent kinase 1 (CDK1) are important for the process. For instance, CDK1 activity triggers both lamin and NPC depolymerization (Guttinger et al., 2009; Heald and McKeon, 1990; Onischenko et al., 2005; Peter et al., 1990). In addition, the polo-like kinase PLK1 contributes to NEBD in several species including *Caernohabditis elegans* (Chase et al., 2000; Rahman et al., 2015) and human (Lenart et al., 2007). The fission yeast SPB is known to integrate input from kinase cascades that trigger mitosis; for instance, the SPB component Cut12 shows a network of genetic interactions with CDK (Cdc2)(Grallert et al., 2013). While these events are thought of as largely cytoplasmic, there is also evidence suggesting Cdc2 localization to the nuclear face of the NE beneath the SPB

(Alfa et al., 1990). In mitotic interphase, 30–40% of Cdc2 signal appears to be nuclear (Decottignies et al., 2001); its colocalization with SPBs could reflect cytoplasmic SPB interactions and/or centromere interactions. Moreover, during meiotic prophase, Cdc2 localizes not only to the SPB (Hou H and JPC, unpublished data), but also to the dissociated centromeres (Decottignies et al., 2001), suggesting a chromatin-based mechanism of localizing CDK in the vicinity of the SPB; such concentration of kinase activity could be envisioned to promote NE fenestration *via* phosphorylation of NE components. These ideas are under investigation.

As bipolar spindle formation involves not only NE fenestration, but also modifications of the SPB that enable it to insert and nucleate spindle microtubules, the failure of all these processes upon destruction of centromere-LINC contacts could reflect one or a series of roles. For instance, centromere-LINC contacts may lead to modification of multiple players in NE fenestration and SPB activation. Alternatively, centromere-LINC contacts may act solely in triggering the NE remodeling events required for fenestration, without which the SPB can neither insert nor engage nuclear γ-TUC to nucleate spindle formation. Our observation that the new SPB is more sensitive than the old SPB to meiotic bouquet disruption (Figure S1I) at first glance might favor the idea that direct modifications specific to the new SPB depend on telomere/centromere-LINC contacts. However, it is also conceivable that NE remodeling processes are so spatially restricted that fenestration can occur beneath the old SPB while the NE remains intact beneath the new SPB, preventing its insertion.

The *sad1.2* phenotype is unique among mutations thus far reported to thwart SPB insertion and/or bipolar spindle formation. For instance, the transmembrane protein Cut11 localizes both to NPCs and the mitotic SPB, where it has been proposed to generate a physical interface between the NE and the proteinaceous SPB as it inserts (Tamm et al., 2011; West et al., 1998). In *cut11.1* cells, the new SPB fails to nucleate microtubules, leading to monopolar spindle formation; moreover, while NE breakdown occurs, this SPB fails to insert properly, leading to NE interruptions seen *via* EM, leakage of nuclear contents into the cytoplasm, and SPBs sinking into the nucleoplasm upon mitotic onset. While the *sad1.2* phenotype resembles that of *cut11.1* in preventing SPBs from nucleating spindle microtubules, nuclear efflux is never seen and the SPBs of *sad1.2* cells (and bouquet-deficient meiotic cells) do not sink into the nucleus but rather, dislodge outward from the NE to the cytoplasm. This curious behavior, seen only after SPB duplication, suggests that some pre-fenestration SPB transitions or NE remodeling events occur in the *sad1.2* setting while others fail, leading to loss of the hydrophobic interface that connects SPBs to the outer NE.

The coupling we observe between intra-nuclear events and the SPB has precedent in observations that mammalian centrosome duplication as well as centriolar disengagement are controlled by proteins with key roles in chromosome replication and segregation inside the nucleus. In particular, origin recognition complex proteins have been implicated in the control of centrosome duplication, and separase, the protein responsible for dissolving cohesion between sister chromatids, in centriolar disengagement (Hemerly et al., 2009; Prasanth et al., 2004; Schockel et al., 2011; Stuermer et al., 2007; Tsou et al., 2009). Whether centromeres, telomeres or other chromosomal landmarks control the onset of

mammalian NEBD has yet to be determined. Indeed, our results highlight the need to investigate LINC associations with specific mammalian chromosome regions during interphase, as the existence of modules that integrate NEBD, spindle formation and chromosome state is likely to be conserved.

Experimental Procedures

Construction of truncated *sad1* alleles and isolation of temperature-sensitive *sad1.2* mutant

The nucleoplasmic portion of Sad1 was divided into 11 subregions (A-K), and diploid strains heterozygous for deletion of each region were constructed. To generate truncated Sad1 alleles, *sad1+-GFP* was cloned into pFA6a-kanMX6 plasmid and used as template for QuickChange II XL kit site-directed mutagenesis (Agilent Technologies). Mutagenic primer design was carried out using the www.agilent.com/genomics/qcpd. Sad1-GFP alleles were amplified using Long Expand Template polymerase (Roche). To query the importance of each Sad1 region for interphase centromere-LINC clustering, we visualized centromeres *via* Mis6 (endogenously tagged with GFP), the SPB *via* Sid4 (endogenously tagged with mCherry) and ectopically expressed tubulin (mCherry-Atb2). Mutagenic PCR on the region encoding amino acids 2–60 was performed using primers 500 bp upstream and 280 bp downstream of the *sad1* ORF, unbalanced dNTP conditions (2.5 mM dGTP, 0.25 mM dATP, dCTP and dTTP) and Vent DNA polymerase (NEB). *wt* haploid cells were transformed with DNA fragments containing the mutagenized *sad1* products and plated on YE4S+ Kan media at 25 °C, then replica plated at 36 °C. Of 10,000 colonies screened those showing temperature-sensitive growth and stable Sad1-GFP signal at the SPB were sequenced. To confirm that *sad1.2* confers this phenotype, Sad1.2 mutations as well as alternatives substitutions of threonine at position 3 and/or alanine at position 52 were generated using the QuickChange II XL kit site-directed mutagenesis (Agilent Technologies).

Quantitation of fluorescence intensity

Sad1, Sid4, Cut11, Cut12 and Pcp1 signal quantitation were performed using Volocity and ImageJ software on images acquired over 26 focal planes at a 0.35 μm step size at each time point. Images were deconvolved and combined into a 2D image using SoftWorx (Applied Precision). For each time point, the intensity of the area containing a given signal was quantified and that of an equivalent signal-free region within the same cell subtracted; and the resulting signal intensities were normalized to the average intensity for one pixel of background outside the cell.

Electron tomography

Tomography was performed to reconstruct spindles as described previously (Grishchuk and McIntosh, 2006; Hoog et al., 2007). Briefly, 15-nm colloidal gold particles (Sigma-Aldrich) were attached to each surface of the semi-thick sections to serve as fiducial markers for subsequent image alignment. Dual axis tilt series datasets were imaged using a TECNAI TF30 intermediate-voltage electron microscope (FEI Corporation; Hillsboro, Oregon) operated at 300 kV. The SerialEM program (Mastronarde, 2005), was used to automatically acquire images every 1.5° over a ± 60° range using a Gatan Ultrascan camera at a pixel size

of 1–1.2 nm. Tomograms from 3–6 serial sections were calculated using the IMOD software package and joined to produce a final volume containing the complete spindle (Kremer et al., 1996; Mastronarde, 1997).

Tomograms were displayed and analyzed using the IMOD program, 3dmod (Kremer et al., 1996). Spindle microtubules originating from either pole were modeled in green and pink, respectively, and the position of their plus ends marked with a blue sphere. In some models, cytoplasmic microtubules were modeled in light blue.

Further details on methods can be found in the Supplementary Experimental Procedures.

Supplementary Material

Refer to Web version on PubMed Central for supplementary material.

Acknowledgments

References

Alfa CE, Ducommun B, Beach D, Hyams JS. Distinct nuclear and spindle pole body population of cyclin-cdc2 in fission yeast. Nature. 1990; 347:680–682. [PubMed: 1699136]

Asakawa H, Hayashi A, Haraguchi T, Hiraoka Y. Dissociation of the Nuf2-Ndc80 complex releases centromeres from the spindle-pole body during meiotic prophase in fission yeast. Mol biol cell. 2005; 16:2325–2338. [PubMed: 15728720]

Basto R, Brunk K, Vinadogrova T, Peel N, Franz A, Khodjakov A, Raff JW. Centrosome amplification can initiate tumorigenesis in flies. Cell. 2008; 133:1032–1042. [PubMed: 18555779]

Bettencourt-Dias M, Glover DM. Centrosome biogenesis and function: centrosomics brings new understanding. Nature reviews Mol cell biol. 2007; 8:451–463.

Bridge AJ, Morphew M, Bartlett R, Hagan IM. The fission yeast SPB component Cut12 links bipolar spindle formation to mitotic control. Genes & dev. 1998; 12:927–942. [PubMed: 9531532]

Carpy A, Krug K, Graf S, Koch A, Popic S, Hauf S, Macek B. Absolute proteome and phosphoproteome dynamics during the cell cycle of Schizosaccharomyces pombe. Mol cell proteomics: MCP. 2014; 13:1925–1936. [PubMed: 24763107]

Chang L, Gould KL. Sid4p is required to localize components of the septation initiation pathway to the spindle pole body in fission yeast. Proc Nat Acad Sci. 2000; 97:5249–5254. [PubMed: 10805785]

Chase D, Serafinas C, Ashcroft N, Kosinski M, Longo D, Ferris DK, Golden A. The polo-like kinase PLK-1 is required for nuclear envelope breakdown and the completion of meiosis in Caenorhabditis elegans. Genesis. 2000; 26:26–41. [PubMed: 10660671]

Chikashige Y, Tsutsumi C, Yamane M, Okamasa K, Haraguchi T, Hiraoka Y. Meiotic proteins bqt1 and bqt2 tether telomeres to form the bouquet arrangement of chromosomes. Cell. 2006; 125:59–69. [PubMed: 16615890]

Cooper JP, Watanabe Y, Nurse P. Fission yeast Taz1 protein is required for meiotic telomere clustering and recombination. Nature. 1998; 392:828–831. [PubMed: 9572143]

De Souza CP, Osmani AH, Hashmi SB, Osmani SA. Partial nuclear pore complex disassembly during closed mitosis in Aspergillus nidulans. Curr biol. 2004; 14:1973–1984. [PubMed: 15556859]

Decottignies A, Zarzov P, Nurse P. In vivo localisation of fission yeast cyclin-dependent kinase cdc2p and cyclin B cdc13p during mitosis and meiosis. J cell sci. 2001; 114:2627–2640. [PubMed: 11683390]

Ding DQ, Chikashige Y, Haraguchi T, Hiraoka Y. Oscillatory nuclear movement in fission yeast meiotic prophase is driven by astral microtubules, as revealed by continuous observation of chromosomes and microtubules in living cells. J cell sci. 1998; 111(Pt 6):701–712. [PubMed: 9471999]

Ding R, West RR, Morphew DM, Oakley BR, McIntosh JR. The spindle pole body of Schizosaccharomyces pombe enters and leaves the nuclear envelope as the cell cycle proceeds. Mol biol cell. 1997; 8:1461–1479. [PubMed: 9285819]

Fennell A, Fernandez-Alvarez A, Tomita K, Cooper JP. Telomeres and centromeres have interchangeable roles in promoting meiotic spindle formation. J cell biol. 2015; 208:415–428. [PubMed: 25688135]

Flory MR, Morphew M, Joseph JD, Means AR, Davis TN. Pcp1p, an Spc110p-related calmodulin target at the centrosome of the fission yeast Schizosaccharomyces pombe. Cell growth & differentiation: the molecular biology journal of the American Association for Cancer Research. 2002; 13:47–58. [PubMed: 11864908]

Folco HD, Pidoux AL, Urano T, Allshire RC. Heterochromatin and RNAi are required to establish CENP-A chromatin at centromeres. Science. 2008; 319:94–97. [PubMed: 18174443]

Fong CS, Sato M, Toda T. Fission yeast Pcp1 links polo kinase729 mediated mitotic entry to gamma-tubulin-dependent spindle formation. EMBO j. 2010; 29:120–130. [PubMed: 19942852]

Friederichs JM, Ghosh S, Smoyer CJ, McCroskey S, Miller BD, Weaver KJ, Delventhal KM, Unruh J, Slaughter BD, Jaspersen SL. The SUN protein Mps3 is required for spindle pole body insertion into the nuclear membrane and nuclear envelope homeostasis. PLoS genet. 2011; 7:e1002365. [PubMed: 22125491]

Funabiki H, Hagan I, Uzawa S, Yanagida M. Cell cycle-dependent specific positioning and clustering of centromeres and telomeres in fission yeast. J cell biol. 1993; 121:961–976. [PubMed: 8388878]

Funaya C, Samarasinghe S, Pruggnaller S, Ohta M, Connolly Y, Muller J, Murakami H, Grallert A, Yamamoto M, Smith D, et al. Transient structure associated with the spindle pole body directs meiotic microtubule reorganization in S. pombe. Curr biol. 2012; 22:562–574. [PubMed: 22425159]

Ganem NJ, Godinho SA, Pellman D. A mechanism linking extra centrosomes to chromosomal instability. Nature. 2009; 460:278–282. [PubMed: 19506557]

Gonczy P. Centrosomes and cancer: revisiting a long-standing relationship. Nature reviews Cancer. 2015; 15:639–652. [PubMed: 26493645]

Gould RR, Borisy GG. The pericentriolar material in Chinese hamster ovary cells nucleates microtubule formation. J cell biol. 1977; 73:601–615. [PubMed: 559676]

Grallert A, Krapp A, Bagley S, Simanis V, Hagan IM. Recruitment of NIMA kinase shows that maturation of the S. pombe spindle-pole body occurs over consecutive cell cycles and reveals a role for NIMA in modulating SIN activity. Genes & dev. 2004; 18:1007–1021. [PubMed: 15132994]

Grallert A, Patel A, Tallada VA, Chan KY, Bagley S, Krapp A, Simanis V, Hagan IM. Centrosomal MPF triggers the mitotic and morphogenetic switches of fission yeast. Nature cell biol. 2013; 15:88–95. [PubMed: 23222840]

Grishchuk EL, McIntosh JR. Microtubule depolymerization can drive poleward chromosome motion in fission yeast. EMBO j. 2006; 25:4888–4896. [PubMed: 17036054]

Guttinger S, Laurell E, Kutay U. Orchestrating nuclear envelope disassembly and reassembly during mitosis. Nature reviews Mol cell biol. 2009; 10:178–191.

Hagan I, Yanagida M. The product of the spindle formation gene sad1+ associates with the fission yeast spindle pole body and is essential for viability. J cell biol. 1995; 129:1033–1047. [PubMed: 7744953]

Heald R, McKeon F. Mutations of phosphorylation sites in lamin A that prevent nuclear lamina disassembly in mitosis. Cell. 1990; 61:579–589. [PubMed: 2344612]

Hemerly AS, Prasanth SG, Siddiqui K, Stillman B. Orc1 controls centriole and centrosome copy number in human cells. Science. 2009; 323:789–793. [PubMed: 19197067]

Hoog JL, Schwartz C, Noon AT, O'Toole ET, Mastronarde DN, McIntosh JR, Antony C. Organization of interphase microtubules in fission yeast analyzed by electron tomography. Dev cell. 2007; 12:349–361. [PubMed: 17336902]

Hou H, Zhou Z, Wang Y, Wang J, Kallgren SP, Kurchuk T, Miller EA, Chang F, Jia S. Csi1 links centromeres to the nuclear envelope for centromere clustering. J cell biol. 2012; 199:735–744. [PubMed: 23166349]

Jaspersen SL, Ghosh S. Nuclear envelope insertion of spindle pole bodies and nuclear pore complexes. Nucleus. 2012; 3:226–236. [PubMed: 22572959]

Jin Y, Mancuso JJ, Uzawa S, Cronembold D, Cande WZ. The fission yeast homolog of the human transcription factor EAP30 blocks meiotic spindle pole body amplification. Dev cell. 2005; 9:63–73. [PubMed: 15992541]

Job D, Valiron O, Oakley B. Microtubule nucleation. Curr opin cell biol. 2003; 15:111–117. [PubMed: 12517712]

Katsani KR, Karess RE, Dostatni N, Doye V. In vivo dynamics of Drosophila nuclear envelope components. Mol biol cell. 2008; 19:3652–3666. [PubMed: 18562695]

Kiseleva E, Rutherford S, Cotter LM, Allen TD, Goldberg MW. Steps of nuclear pore complex disassembly and reassembly during mitosis in early Drosophila embryos. J cell sci. 2001; 114:3607–3618. [PubMed: 11707513]

Klutstein M, Cooper JP. The Chromosomal Courtship Dance-homolog pairing in early meiosis. Curr opin cell biol. 2014; 26C:123–131.

Klutstein M, Fennell A, Fernandez-Alvarez A, Cooper JP. The telomere bouquet regulates meiotic centromere assembly. Nature cell biol. 2015; 17:458–469. [PubMed: 25774833]

Kremer JR, Mastronarde DN, McIntosh JR. Computer visualization of three-dimensional image data using IMOD. J struc biol. 1996; 116:71–76.

Lenart P, Petronczki M, Steegmaier M, Di Fiore B, Lipp JJ, Hoffmann M, Rettig WJ, Kraut N, Peters JM. The small-molecule inhibitor BI 2536 reveals novel insights into mitotic roles of polo-like kinase 1. Curr biol. 2007; 17:304–315. [PubMed: 17291761]

Lim HH, Zhang T, Surana U. Regulation of centrosome separation in yeast and vertebrates: common threads. Trends cell biol. 2009; 19:325–333. [PubMed: 19576775]

Makarova M, Oliferenko S. Mixing and matching nuclear envelope remodeling and spindle assembly strategies in the evolution of mitosis. Curr opin cell biol. 2016; 41:43–50. [PubMed: 27062548]

Mardin BR, Schiebel E. Breaking the ties that bind: new advances in centrosome biology. J cell biol. 2012; 197:11–18. [PubMed: 22472437]

Mastronarde DN. Dual-axis tomography: an approach with alignment methods that preserve resolution. J struc biol. 1997; 120:343–352.

Mastronarde DN. Automated electron microscope tomography using robust prediction of specimen movements. J struc biol. 2005; 152:36–51.

McCully EK, Robinow CF. Mitosis in the fission yeast Schizosaccharomyces pombe: a comparative study with light and electron microscopy. J Cell Sci. 1971; 9:475–507. [PubMed: 4108061]

Ohta M, Sato M, Yamamoto M. Spindle pole body components are reorganized during fission yeast meiosis. Mol biol cell. 2012; 23:1799–1811. [PubMed: 22438582]

Onischenko EA, Gubanova NV, Kiseleva EV, Hallberg E. Cdk1 and okadaic acid-sensitive phosphatases control assembly of nuclear pore complexes in Drosophila embryos. Mol biol cell. 2005; 16:5152–5162. [PubMed: 16120647]

Paddy MR, Saumweber H, Agard DA, Sedat JW. Time-resolved, in vivo studies of mitotic spindle formation and nuclear lamina breakdown in Drosophila early embryos. J cell sci. 1996; 109:591–607. [PubMed: 8907705]

Pereira G, Tanaka TU, Nasmyth K, Schiebel E. Modes of spindle pole body inheritance and segregation of the Bfa1p-Bub2p checkpoint protein complex. EMBO j. 2001; 20:6359–6370. [PubMed: 11707407]

Peter M, Nakagawa J, Doree M, Labbe JC, Nigg EA. In vitro disassembly of the nuclear lamina and M phase-specific phosphorylation of lamins by cdc2 kinase. Cell. 1990; 61:591–602. [PubMed: 2188731]

Petronczki M, Siomos MF, Nasmyth K. Un menage a quatre: the molecular biology of chromosome segregation in meiosis. Cell. 2003; 112:423–440. [PubMed: 12600308]

Pfender S, Kuznetsov V, Pasternak M, Tischer T, Santhanam B, Schuh M. Live imaging RNAi screen reveals genes essential for meiosis in mammalian oocytes. Nature. 2015; 524:239–242. [PubMed: 26147080]

Prasanth SG, Prasanth KV, Siddiqui K, Spector DL, Stillman B. Human Orc2 localizes to centrosomes, centromeres and heterochromatin during chromosome inheritance. EMBO j. 2004; 23:2651–2663. [PubMed: 15215892]

Rahman MM, Munzig M, Kaneshiro K, Lee B, Strome S, Muller-Reichert T, Cohen-Fix O. Caenorhabditis elegans polo-like kinase PLK-1 is required for merging parental genomes into a single nucleus. Mol biol cell. 2015; 26:4718–4735. [PubMed: 26490119]

Rothbauer U, Zolghadr K, Tillib S, Nowak D, Schermelleh L, Gahl A, Backmann N, Conrath K, Muyldermans S, Cardoso MC, et al. Targeting and tracing antigens in live cells with fluorescent nanobodies. Nature methods. 2006; 3:887–889. [PubMed: 17060912]

Sazer S, Lynch M, Needleman D. Deciphering the evolutionary history of open and closed mitosis. Current biology: CB. 2014; 24:R1099–1103. [PubMed: 25458223]

Scherthan H. A bouquet makes ends meet. Nature reviews Mol cell biol. 2001; 2:621–627.

Schockel L, Mockel M, Mayer B, Boos D, Stemmann O. Cleavage of cohesin rings coordinates the separation of centrioles and chromatids. Nature cell biol. 2011; 13:966–972. [PubMed: 21743463]

Smoyer CJ, Jaspersen SL. Breaking down the wall: the nuclear envelope during mitosis. Curr opin cell biol. 2014; 26:1–9. [PubMed: 24529240]

Stafstrom JP, Staehelin LA. Dynamics of the nuclear envelope and of nuclear pore complexes during mitosis in the Drosophila embryo. European j cell biol. 1984; 34:179–189. [PubMed: 6428889]

Stuermer A, Hoehn K, Faul T, Auth T, Brand N, Kneissl M, Putter V, Grummt F. Mouse pre-replicative complex proteins colocalise and interact with the centrosome. European j cell biol. 2007; 86:37–50. [PubMed: 17157410]

Takahashi K, Chen ES, Yanagida M. Requirement of Mis6 centromere connector for localizing a CENP-A-like protein in fission yeast. Science. 2000; 288:2215–2219. [PubMed: 10864871]

Tallada VA, Tanaka K, Yanagida M, Hagan IM. The S. pombe mitotic regulator Cut12 promotes spindle pole body activation and integration into the nuclear envelope. J cell biol. 2009; 185:875–888. [PubMed: 19487457]

Tamm T, Grallert A, Grossman EP, Alvarez-Tabares I, Stevens FE, Hagan IM. Brr6 drives the Schizosaccharomyces pombe spindle pole body nuclear envelope insertion/extrusion cycle. J cell biol. 2011; 195:467–484. [PubMed: 22042620]

Tanaka K, Kanbe T. Mitosis in the fission yeast Schizosaccharomyces pombe as revealed by freeze-substitution electron microscopy. J cell sci. 1986; 80:253–268. [PubMed: 3522614]

Tanaka K, Kohda T, Yamashita A, Nonaka N, Yamamoto M. Hrs1p/Mcp6p on the meiotic SPB organizes astral microtubule arrays for oscillatory nuclear movement. Curr biol. 2005; 15:1479–1486. [PubMed: 16111942]

Tomita K, Bez C, Fennell A, Cooper JP. A single internal telomere tract ensures meiotic spindle formation. EMBO reports. 2013; 14:252–260. [PubMed: 23295325]

Tomita K, Cooper JP. The telomere bouquet controls the meiotic spindle. Cell. 2007; 130:113–126. [PubMed: 17632059]

Tsou MF, Wang WJ, George KA, Uryu K, Stearns T, Jallepalli PV. Polo kinase and separase regulate the mitotic licensing of centriole duplication in human cells. Dev cell. 2009; 17:344–354. [PubMed: 19758559]

Vardy L, Toda T. The fission yeast gamma-tubulin complex is required in G(1) phase and is a component of the spindle assembly checkpoint. EMBO j. 2000; 19:6098–6111. [PubMed: 11080156]

West RR, Vaisberg EV, Ding R, Nurse P, McIntosh JR. cut11(+): A gene required for cell cycle-dependent spindle pole body anchoring in the nuclear envelope and bipolar spindle formation in Schizosaccharomyces pombe. Mol biol of cell. 1998; 9:2839–2855. [PubMed: 9763447]

Witkin KL, Friederichs JM, Cohen-Fix O, Jaspersen SL. Changes in the nuclear envelope environment affect spindle pole body duplication in Saccharomyces cerevisiae. Genetics. 2010; 186:867–883. [PubMed: 20713690]

Yanowitz J. Meiosis: making a break for it. Curr opin cell biol. 2010; 22:744–751. [PubMed: 20829015]

Yoshida M, Sazer S. Nucleocytoplasmic transport and nuclear envelope integrity in the fission yeast Schizosaccharomyces pombe. Methods. 2004; 33:226–238. [PubMed: 15157890]

Highlights

- Mitotic and meiotic spindle formation require prior chromosome-LINC contact.

- Sad1.2 maintains LINC stability but destroys interphase centromere-LINC contact.

- Partial nuclear envelope breakdown is lost in *sad1.2* cells.

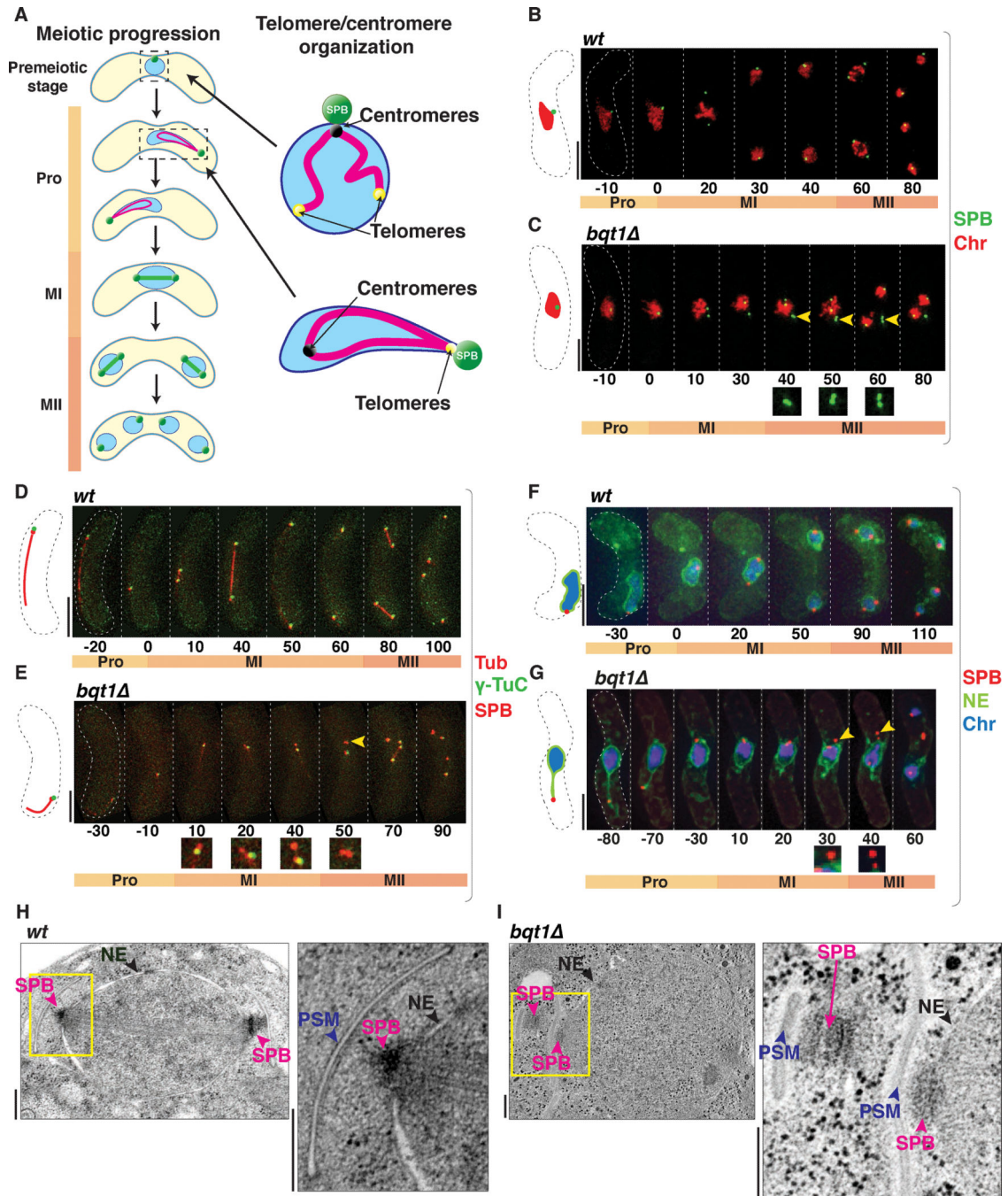- Chromosome-LINC interactions control spindle *via* nuclear envelope regulation.

Figure 1. SPBs fail to insert into the NE in the absence of the bouquet

(A) Schematic of meiotic chromosomal organization. During prophase (Pro), the nucleus oscillates, pulled by the SPB, then settles prior to MI onset. Homolog separation at MI followed by sister segregation at MII leads to haploid spores. Right: In mitotic interphase, centromeres cluster beneath the SPB; in meiotic prophase, telomeres cluster there to form the bouquet. (B–G) Frames from films of meiosis. Numbers underneath represent time (minutes) from MI onset. In all light microscopy images in all figures, scale bars equal 5 μm. (B–C) The SPB is viewed *via* Pcp1-GFP (endogenously tagged), chromatin (Chr) *via* Hht1-

mRFP (histone H3 tagged at one of the two endogenous *hht1⁺* loci). Yellow arrowheads point to SPBs failing to separate. (D–E) SPBs viewed *via* endogenously tagged Sid4-mRFP, γ-TuC *via* Alp4-GFP, and tubulin (Tub) *via* ectopically expressed mRFP-Atb2. (D) The γ-TuC localizes to the SPB throughout *wt* meiosis (Tanaka et al., 2005). (E) In *bqt1* meiosis, some SPBs lack visible γ-TuC (yellow arrowhead). (F–G) Tags as above with *nmt1*-controlled Ish1-GFP to visualize the NE. In *bqt1* cells, the SPB separates from the NE (yellow arrowheads). See also Figure S1. (H–I) EM of MII nuclei. Yellow boxes are magnified to the right. Prospore membranes (PSM) are seen adjacent to SPBs, confirming that cells are in MII. Scale bars represent 200 nm. While *wt* SPBs insert into the NE and nucleate microtubules (H), the upper left SPB in (I) has failed to insert and has been displaced into the cytoplasm. See also Figure S2.
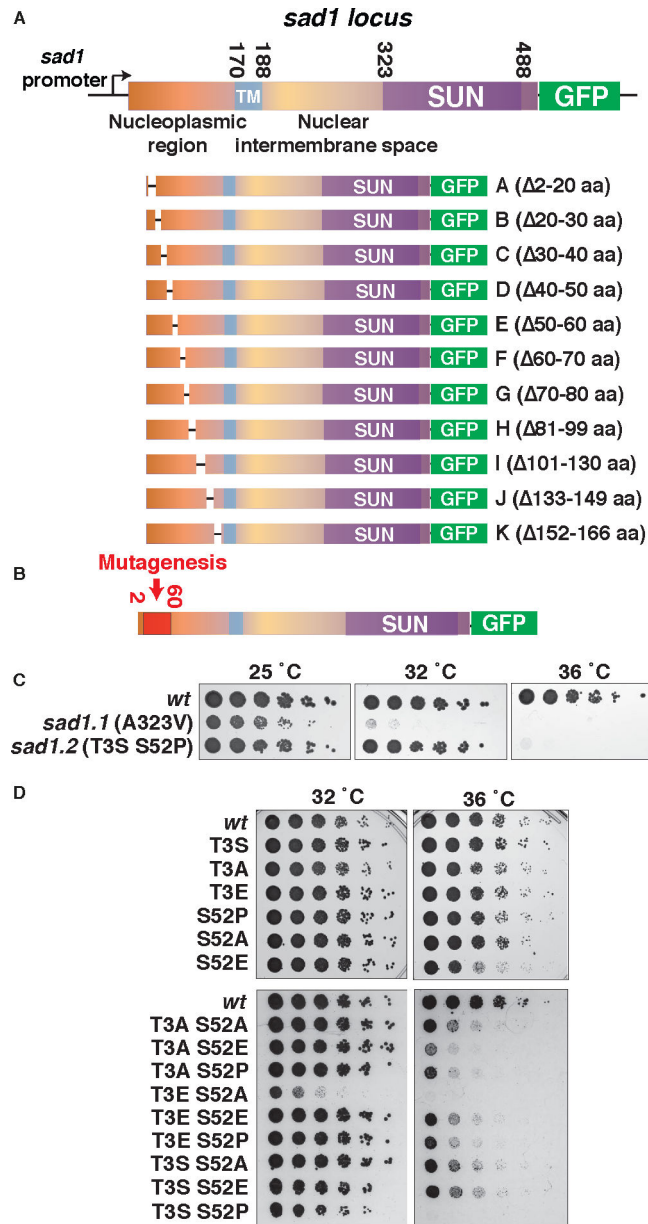
Figure 2. Development of conditional allele, *sad1.2*

(A) Schematic of *sad1* alleles with deletions in the nucleoplasmic domain. Transmembrane domain (TM) and SUN-domain are indicated. Each deletion allele replaced *sad1+* and was GFP tagged. (B) The region subjected to PCR mutagenesis (2–60 aa) is indicated; see also Figure S3. (C) *sad1.2* confers temperature sensitivity. Serial dilution (fivefold) of log-phase cultures (0.8×10^7 cells/mL) were spotted and grown on rich media. (D) Targeted mutations abolishing or mimicking phosphorylation at the two sites mutated in *sad1.2* were used to replace *wt sad1+* as in (A). Phosphorylation alone cannot account for *sad1.2* temperature sensitivity.
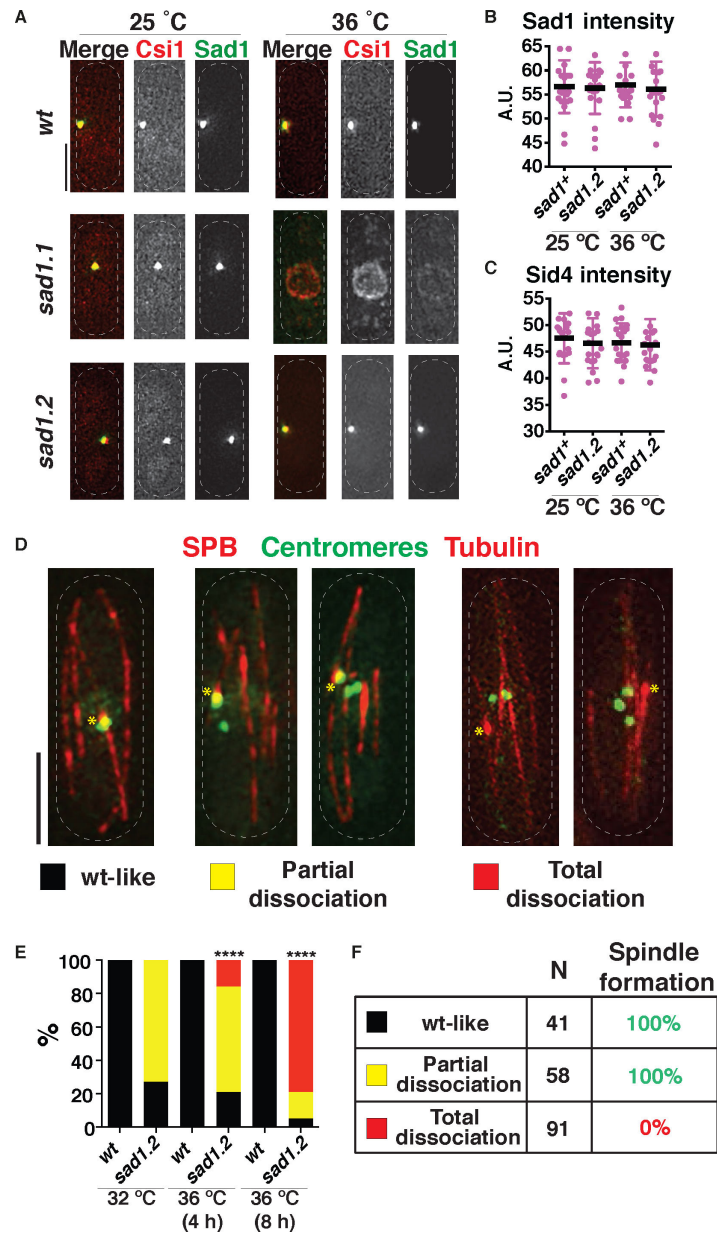
Figure 3. Complete centromere dissociation from the LINC complex during interphase results in spindle failure

(A–C) The SPB remains intact in *sad1.2* cells at restrictive temperature. (A) Csi1 localization is abolished in *sad1.1* cells but unaltered in *sad1.2* cells. Endogenously tagged Csi1-mCherry imaged after 8 h at 36 °C. (B–C) Signal intensities at the SPB during mitotic interphase; n=20 for each genotype. Error bars = standard deviations. (D) Centromere-LINC association patterns during *sad1.2* interphase. Tags as in Figure 1; centromeres imaged *via* endogenously tagged Mis6-GFP. (E) Progressive increase in total centromere-LINC dissociation at 36°C. 100 cells were scored for each condition over more than five independent experiments. Scoring began four frames prior to SPB duplication, with frames taken every 10 min. Mean is shown with bars whose colors correspond to the categories defined in (D). p values were determined by Fisher's exact test (**** = $p < 0.0001$). (F) In

100% of cells harboring one or more centromere-LINC association, proper spindle formation is seen. In contrast, total centromere-LINC dissociation completely abolishes spindle formation. 41, 58 and 91 cells analyzed for *wt-like*, *partial* and *total dissociation* categories, respectively, from 10 independent experiments. Identical results were obtained using other kinetochore markers, again scoring hundreds of cells in 10 independent experiments; see Figure S4.
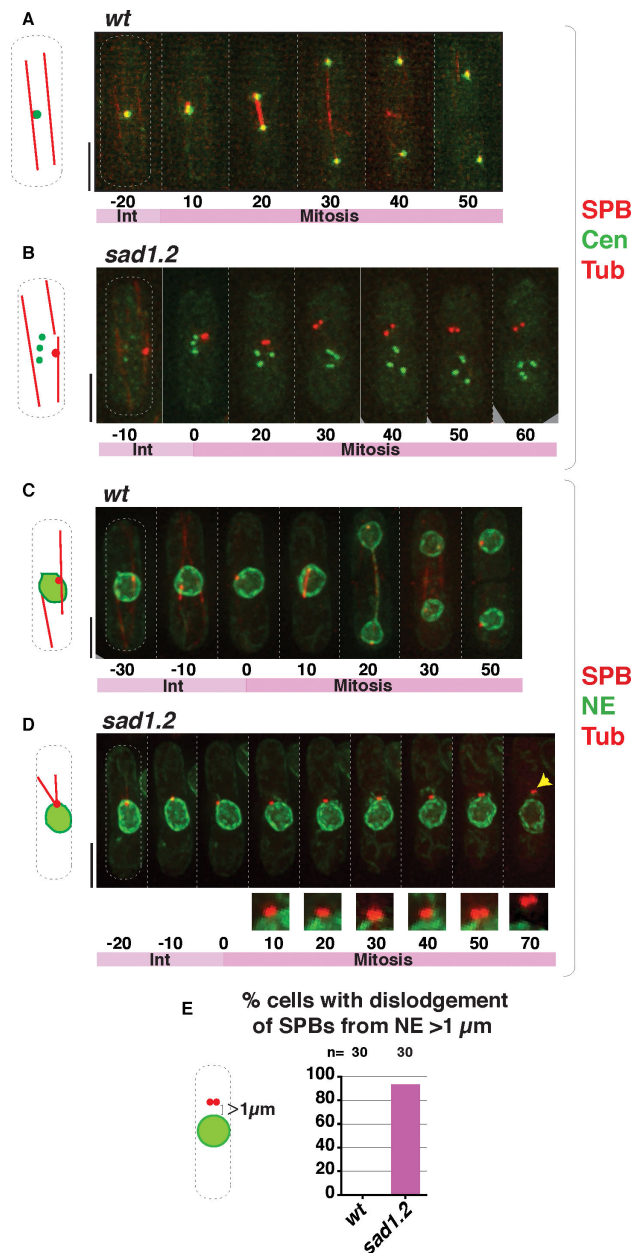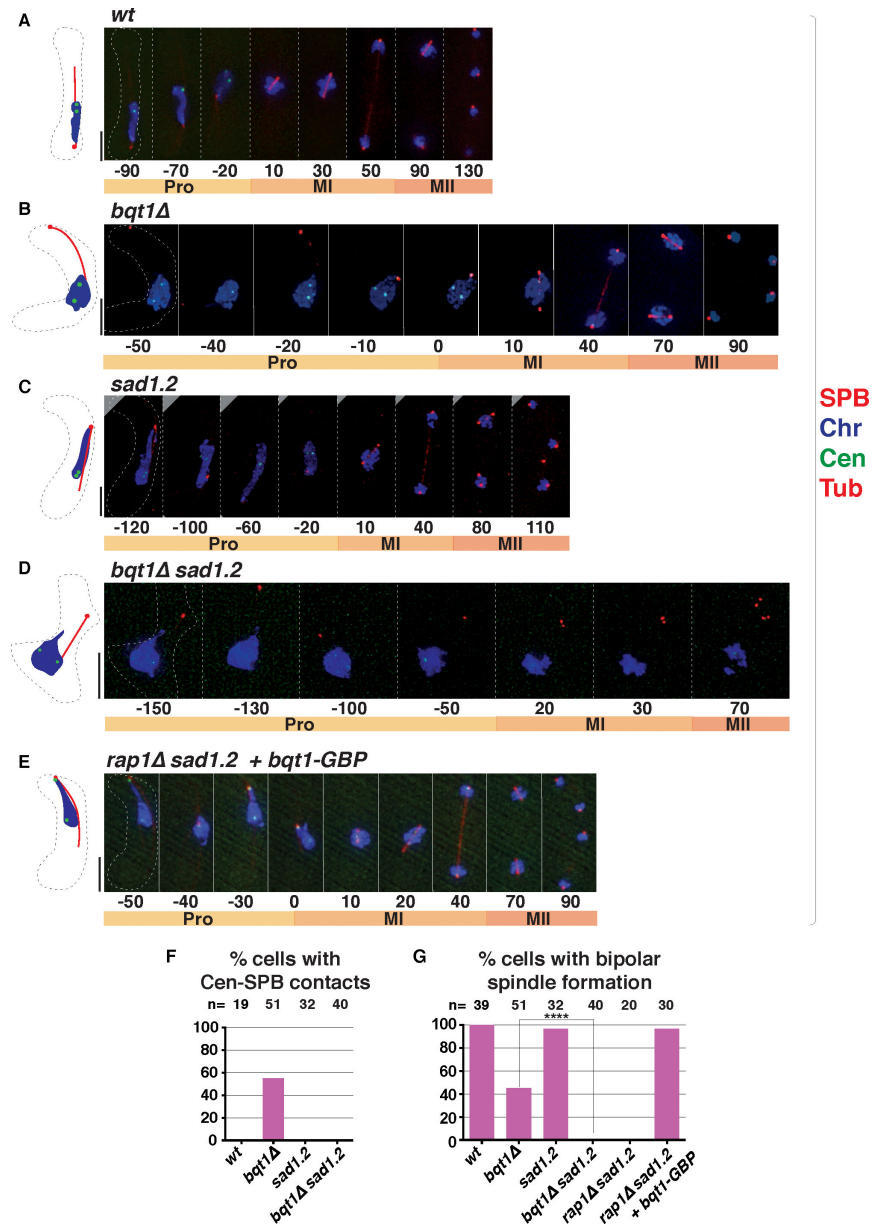
Figure 4. Failed SPB insertion in mitotic *sad1.2* cells leads to abolition of spindle formation
(A–B) Frames from films of proliferating cells at 36 °C; SPBs seen *via* Sid4-mCherry, centromeres *via* Ndc80-GFP (Cen) and spindles *via* ectopically expressed mCherry-Atb2 (*nda3* promoter controlled). Growth for 4 h at 36 °C led to complete centromere-LINC dissociation in the *sad1.2* setting (B); SPB separation defects ensued. (C–D) Visualization of the NE via Ish1-GFP, cells grown as in (A–B). As in *bqt1* meiosis (Figure 1G), the duplicated SPBs detach from NE during *sad1.2* mitosis. Numbers indicate mitotic progression in minutes; t=0 is just before SPB duplication. (E) Quantitation of phenotypes shown in (D) from six independent experiments. Dislodgement of the SPB from the NE is never observed in *wt* cells. *n* is the total number of cells scored. See also Figure S5.
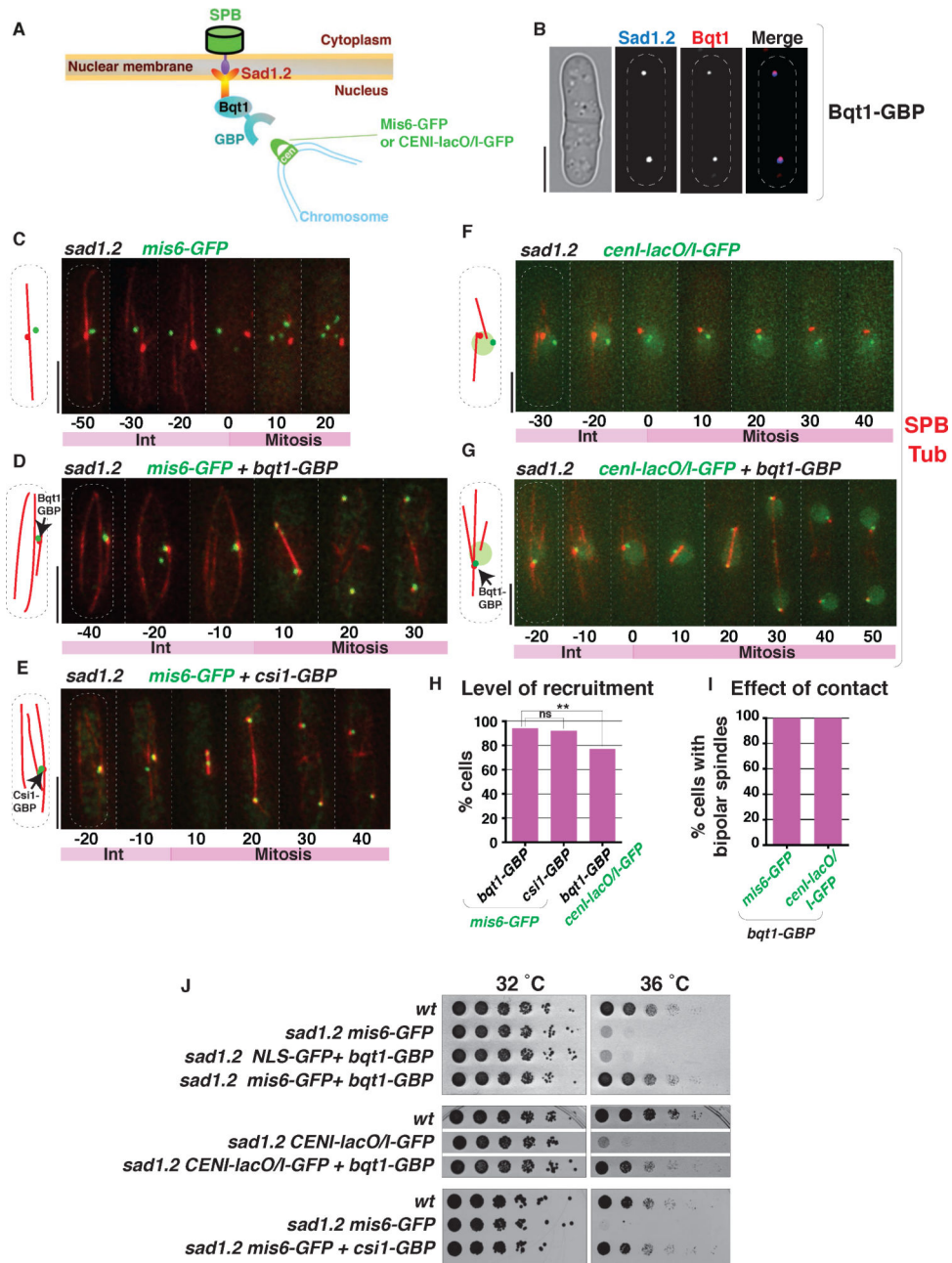
Figure 5. Centromere-SPB interaction and spindle rescue in *bqt1Δ* meiocytes are abolished in a *sad1.2* setting

(A–E) Frames from films of meiosis; tags and numbers as in Figure 1. (F) Meiotic SPB-centromere contacts are abolished by *sad1.2*. (G) Residual MI spindle formation in bouquet-deficient cells is abolished by *sad1.2*. Forced centromere-SPB interaction *via* Bqt1-GBP (see Figure 6A) ensures proper spindle formation. *n* = total number of cells scored in ≥ 5 independent experiments. Data were subjected to Fisher's exact test (**** = $p < 0.0001$).

Figure 6. Forced centromere-Sad1.2 association ensures mitotic spindle formation

(A) Schematic of GFP-GBP system used to force interaction between Sad1.2 and centromeres. *nmt41*-controlled Bqt1-GBP was integrated at the endogenous *bqt1* locus and induced during mitosis; Mis6-GFP was used to recruit centromeres *via* GBP-GFP interaction. (B) Validation of the recruitment system shown in (A). Bqt1-GBP-mCherry localizes to the SPB (visualized with Sad1.2-Turquoise2). (C) In all *sad1.2* cells exhibiting *total centromere dissociation* (n=13) and lacking Bqt1-GBP, spindle formation fails at 36 °C. (D) Bqt1-GBP recruits Mis6-GFP and restores spindle formation at 36 °C in all cases (n=56). (E) As for Bqt1-GBP in (A), Csi1-GBP recruits Mis6-GFP to the SPB, restoring spindle formation in *sad1.2* cells at 36°C in all cases (n=50). (F–G) Spindle formation is also

restored by forcing interaction between centromere-proximal lacO/I-GFP array and the SPB. (H) Quantitation of centromere-SPB recruitment in *sad1.2* cells after 8 hours at 36 °C. 100 cells were quantified in each case. *p* values determined by Fisher's exact test (** = $p < 0.01$). (I) Effect of contact type on spindle formation in *sad1.2* at 36 °C; n=30 cells for each. (J) Serial dilution analysis (as in Figure 2C) shows that ectopic recruitment of a centromere to Sad1.2 rescues growth at restrictive temperature. The deficit in recruitment efficiency conferred by *cenI-lacO/I-GFP* results in a less complete cumulative rescue of viability; however, those cells displaying efficient recruitment uniformly show rescued spindle formation (I).
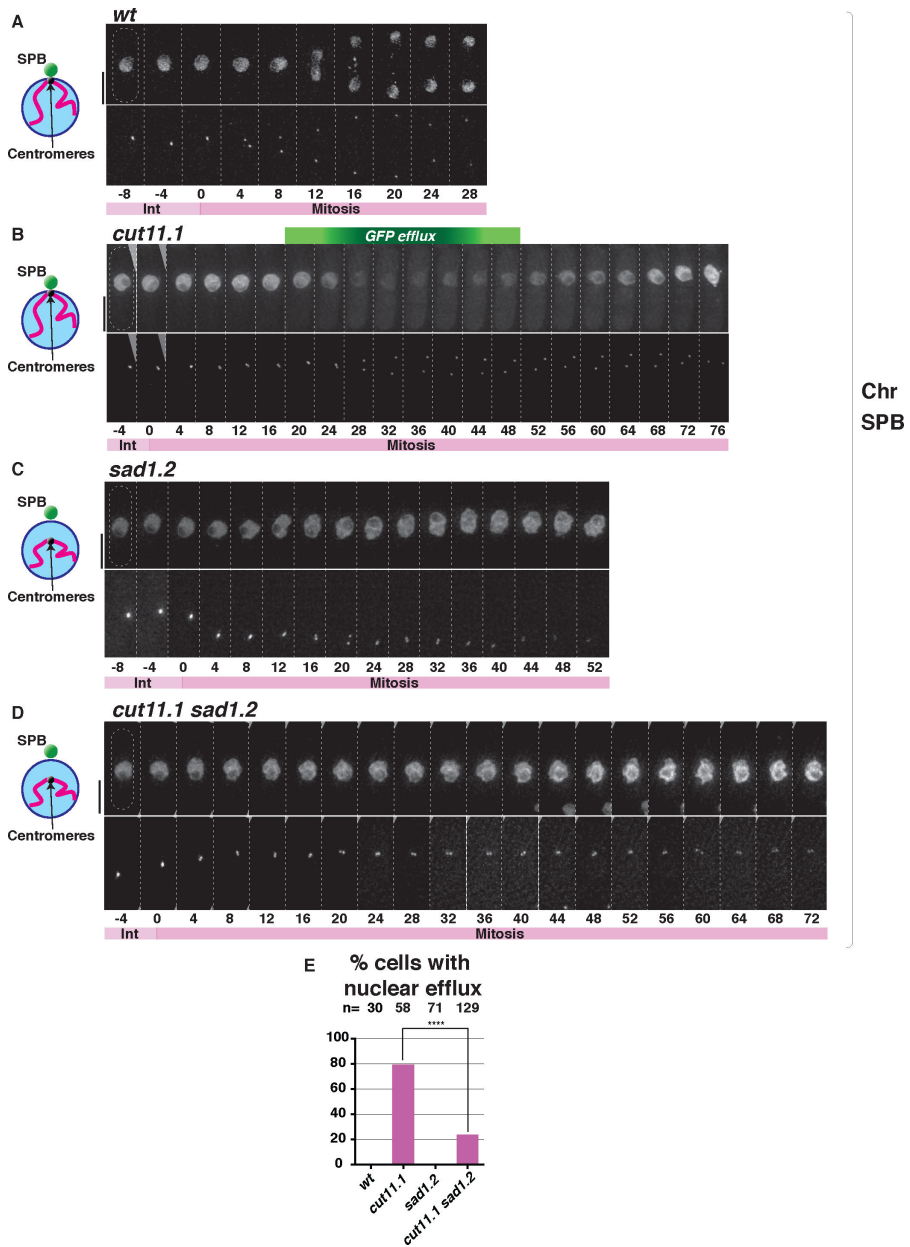
Figure 7. Sad1.2 averts the efflux of nucleoplasm conferred by *cut11.1* mutation

(A–D) NE permeability is monitored *via* efflux of nuclear NLS-GFP-β-Gal in the top row of each pair of panels. Cells harboring Sid4-mCherry (SPB) were grown at 25 °C, shifted to 36 °C and imaged every 4 minutes after 8 hours; t=0 is just before SPB duplication. While NLS-GFP-β-Gal leaks from the nucleus in *cut11.1* cells, it does not in *sad1.2* cells nor *sad1.2 cut11.1* cells, indicating blocked NE fenestration in the *sad1.2* setting. (E) Quantitation of phenotype shown in A–D. *n* = number of cells analyzed in > 5 independent experiments. Data were subjected to Fisher's exact test (**** = $p < 0.0001$). See also Figure S6.